# Bond mobility mechanism in grain boundary embrittlement: First-principles tensile tests of Fe with a P-segregated Σ3 grain boundary

Motohiro Yuasa* and Mamoru Mabuchi
*Department of Energy Science and Technology, Graduate School of Energy Science, Kyoto University, Yoshidahonmachi, Sakyo-ku, Kyoto 606-8501, Japan*
(Received 17 June 2010; published 14 September 2010)

First-principles simulated tensile tests have been performed on Fe with a P-segregated grain boundary to investigate the nature of the bond mobility mechanism in grain boundary embrittlement. The first site for bond breaking was the Fe-P bond, despite its high charge density. This is because the Fe-P bond exhibited the covalentlike characteristics of a localized bonding and the mobility of electrons was reduced. The breaking of the Fe-P bond accelerated the breaking of the Fe-Fe bond around the Fe-P bond because the Fe-P bond breaking affected the electron density of states of the Fe-Fe bond. Thus, P segregation enhanced the grain boundary embrittlement in Fe.

DOI: 10.1103/PhysRevB.82.094108 PACS number(s): 62.20.−x, 68.35.Dv, 81.05.Bx

Grain boundary (GB) embrittlement in metals is often enhanced by impurity segregation at the GB. To date, two mechanisms for the enhancement of GB embrittlement by impurity segregation have been proposed: one is the decohesion mechanism,[1,2] where the metal-metal bond is weakened owing to the charge transfer by impurity atoms, and the other is the bond mobility mechanism,[3–5] where the mobility of electrons is reduced by impurity atoms. Recently, first-principles tensile tests have been performed to investigate the GB embrittlement mechanisms because GB fracture is related not only to the initial electronic state but also to the variation in electronic state with increasing strain.[6–10] For example, Lu *et al.*[9,11] showed that the first bond breaking occurs at the metal-metal bond weakened by the charge transfer. Thus, the decohesion mechanism has been elucidated by first-principles tensile tests.

It is well known that the segregation of P atoms at the GB enhances the intergranular embrittlement in Fe.[12–15] Freeman and colleagues[12,13] showed by first-principles calculations that the intergranular embrittlement enhanced by P segregation is due to the bond mobility mechanism. However, the nature of the bond mobility mechanism is still unknown. It is of interest to investigate whether the bond between the impurity and neighboring host atoms gives rise to its breaking due to the localization or the bond breaking between neighboring host atoms due to the stress concentration caused by the impurity atoms. Recently, first-principles rigid tensile tests of Fe with a P-segregated GB have been performed by Yamaguchi *et al.*[14] However, because the calculations were carried out under the condition that the fracture surface was arbitrarily set between the two atomic layers in the GB, the bond breaking and its related phenomena are still unclear. In the present study, first-principles fully relaxed tensile tests are performed on Fe with a P-segregated GB and with a nonsegregated GB to understand the bond breaking in the bond mobility mechanism.

Two bcc Fe cells with a Σ3 (111)/[1$\bar{1}$0] tilt GB were used: one was the cell without P segregation at the GB (clean GB model) and the other was the cell with P segregation at the GB (P-segregated GB model), in which an Fe atom (Fe2) at the GB was substituted by a P atom, as shown in Fig. 1. The initial cell size was $4.05\times7.02\times14.89$ Å$^3$. Geometry optimization calculations were performed using the Cambridge serial total energy package (CASTEP),[16] in which the density-functional theory[17,18] was used with a plane-wave basis set to calculate the electronic properties of solids from first principles. The exchange-correlation interactions were treated using the spin-polarized version of the generalized gradient approximation within the scheme due to Perdew-Burke-Ernzerhof.[19] The ultrasoft pseudopotentials[20] represented in reciprocal space were used for all elements in the calculations. The Kohn-Sham wave functions of valence electrons were expanded to the plane-wave basis set within a specified cut-off energy (=300 eV). The Brillouin zone was sampled using a Monkhorst-Pack $6\times4\times2$ *k*-point mesh and the Gaussian smearing with 0.1 eV width.

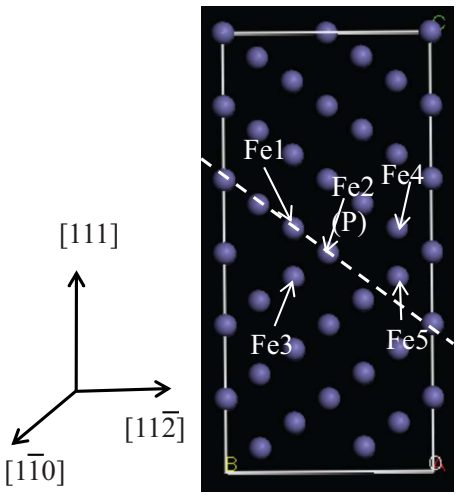


FIG. 1. (Color online) Unit-cell model of Fe with a Σ3 (111)/[1$\bar{1}$0] tilt grain boundary. In the present study, two cells are used: one is the cell without P segregation at the grain boundary (clean GB model) and the other is the cell with P segregation at the grain boundary (P-segregated GB model), in which an Fe atom (Fe2) at the grain boundary is substituted by a P atom. The initial cell size is $4.05\times7.02\times14.89$ Å$^3$. The white dashed line indicates (110) at which the charge density is shown in Fig. 5.

 

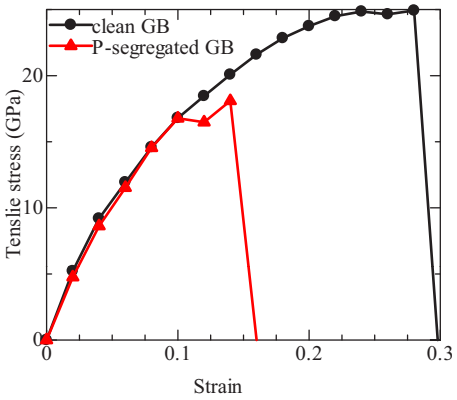


FIG. 2. (Color online) Stress-strain curves of the clean GB and P-segregated GB models calculated by the first-principles tensile tests.

After the geometry optimization calculation including cell optimization, an uniaxial tensile strain with an increment of 2% in the [111] direction, which was normal to the GB plane, was applied to the cells for the first-principles fully relaxed tensile tests. The lattice dimensions in the GB plane were fixed, neglecting Poisson's ratio to simplify the calculation.[8–10] This step was repeated until GB fracture occurred. In each step, all atomic positions were optimized in accordance with Hellman-Feynman forces until all the forces were less than 0.03 eV/Å. In the present study, the bond breaking was determined from a rapid increase in bond length.

The stress-strain curves are shown in Fig. 2 for the clean GB and P-segregated GB models. In the clean GB model, the stress increased up to about 25 GPa with increasing strain until the strain reached 24%. The stress was nearly constant in the strain range of 24–28 %, then the stress rapidly decreased at 28–30 %, and finally, GB fracture occurred at 30%. In the P-segregated GB model, the stress increased up to about 16 GPa until the strain reached 10% and the stress was nearly constant at 10–12 %. After the stress slightly increased at 12–14 %, the stress rapidly decreased at 14–16 %, and finally, GB fracture occurred at 16%. Clearly, P segregation enhanced the GB embrittlement in Fe. According to the Rice-Wang thermodynamics model,[21] an enhancement of GB embrittlement by impurity segregation can be estimated from the difference between the segregation energies at the GB ($=\Delta E_{GB}$) and at the free surface ($=\Delta E_{SF}$). The calculated $\Delta E_{GB}-\Delta E_{SF}$ for the P segregation in Fe was 1.6 eV/atom, which indicates that P is the GB embrittler.[12,13,15] This is in agreement with the results shown in Fig. 2.

The atomic configurations of $(1\bar{1}0)$ at 28% and 30% in the clean GB model and at 10%, 12%, and 16% in the P-segregated GB model are shown in Fig. 3. In the clean GB model, no bond breaking occurred at 28%, and the Fe1-Fe2 and Fe1-Fe3 bonds were broken at 28–30 %. In the P-segregated GB model, the Fe1-P bond was broken at 10–12 %, and the Fe1-Fe3 bond was broken at 12–16 %. These bond-breaking events correspond very well to the stress-strain behavior shown in Fig. 2. Note that the first bond breaking occurred at the Fe1-P bond.

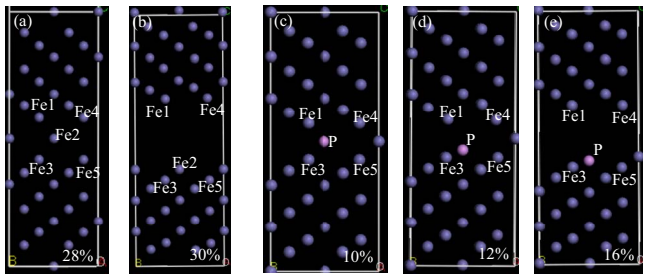


FIG. 3. (Color online) Fully relaxed atomic configuration of $(1\bar{1}0)$, (a) the atomic configuration at 28% in the clean GB model, (b) the atomic configuration at 30% in the clean GB model, (c) the atomic configuration at 10% in the P-segregated GB model, (d) the atomic configuration at 12% in the P-segregated GB model, and (e) the atomic configuration at 16% in the P-segregated GB model. The blue and pink circles indicate the Fe and P atoms, respectively.

Figure 4 shows the charge density isosurfaces of $(1\bar{1}0)$ at the strain of 0%, where the gray and blue regions indicate the charge densities that are higher and lower than the border charge density (=0.32 electrons/Å$^3$), respectively, the black regions between the gray and blue regions indicate charge accumulation due to atomic bonding, and the black regions between the gray regions and between the blue regions indicate charge depletion. A detailed inspection of Fig. 4 reveals that a black region is observed between the Fe1 (Fe3) and P atoms in the P-segregated GB model but no black region is found between the Fe1 (Fe3) and Fe2 atoms in the clean GB model. Also, the isosurface around the P atom in the P-segregated GB model is pentagon shaped while that around the Fe2 atom in the clean GB model is spherical. Thus, the charge density around the P atom in the P-segregated GB model was stronger but more directional than that around the Fe2 atom in the clean GB model.

Figure 5 shows the variations in the charge-density distributions of (110) and $(1\bar{1}0)$ with strain. Although the number of valence electrons of a P atom is less than that of a Fe atom, the charge density of the Fe1-P bond at 0% in the P-segregated GB model is higher than that of the Fe1-Fe2 bond at 0% in the clean GB model. The strong Fe1-P bond

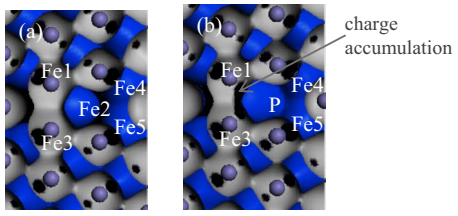


FIG. 4. (Color online) Charge-density isosurfaces of $(1\bar{1}0)$ at the strain of 0%. (a) shows the charge-density isosurface in the clean GB model, and (b), the charge-density isosurface in the P-segregated GB model. The border charge density for the isosurfaces is 0.32 electrons/Å$^3$. The gray and blue regions indicate the charge densities that are higher and the lower than the border charge density, respectively, the black regions between the gray and blue regions indicate the charge accumulation due to atomic bonding, and the black regions between the gray regions and between the blue regions indicate the charge depletion.

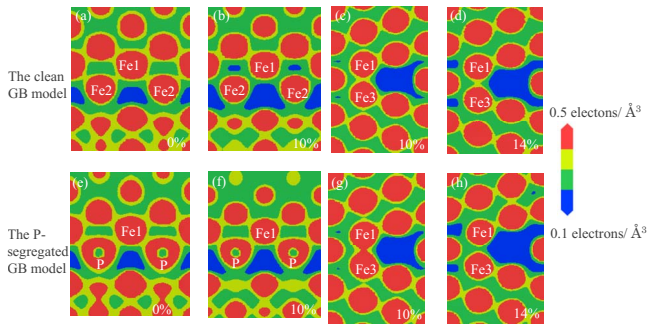


FIG. 5. (Color online) Variations in charge-density distributions of (110) and $(1\bar{1}0)$ with strain. (a) and (b) show the charge-density distributions of (110) at 0% and 10% in the clean GB model, (c) and (d) show the charge-density distributions of $(1\bar{1}0)$ at 10% and 14% in the clean GB model, (e) and (f), the charge-density distributions of (110) at 0% and 10% in the P-segregated GB model, and (g) and (h), the charge-density distributions of $(1\bar{1}0)$ at 10% and 14% in the P-segregated GB model, respectively.

was maintained even at the strain of 10% which was just before it broke. The strong Fe1-P bond is due to the covalentlike characteristics,[12,13,15] as shown later. The Fe1-Fe3 bond at 10% in the P-segregated GB model exhibited a higher charge density than the Fe1-Fe3 bond at 10% in the clean GB model. At the strain of 14%, however, the charge density of the Fe1-Fe3 bond in the P-segregated GB model was reduced significantly by the Fe1-P bond breaking at 10–12 %. Clearly, this Fe1-P bond breaking markedly reduced the charge density of the Fe1-Fe3 bond. On the other hand, the charge density of the Fe1-Fe3 bond at 14% was less reduced in the clean GB model than in the P-segregated GB model. This is because no bond breaking occurred in both the Fe1-Fe2 and Fe2-Fe3 bonds at 14% in the clean GB model.

The variations in bond lengths of the (a) Fe1-Fe2/Fe1-P and (b) Fe1-Fe3 bonds as a function of strain are shown in Fig. 6. The length of the Fe1-P bond was almost constant up to the strain of 10%, and it was shorter than that of the Fe1-Fe2 bond. However, the length of the Fe1-P bond suddenly increased at 12%, showing that the Fe1-P bond breaking occurred at 10–12 %. Thus, the strong Fe1-P bond with a short bond length provided the preferential bond-breaking site. The same trend of preferential breaking of strong bonds has been reported in first-principles calculations on Al.[8,9] In the previous studies,[8,9] the preferential bond breaking was related to a reduction in coordination number at the GB. In the present study, however, the coordination number of the P atom in the P-segregated GB model is the same as that of the Fe2 atom in the clean GB model. As shown in Figs. 4 and 5, the charge density around the P atom is localized and directional, and therefore, the easy breaking of the Fe1-P bond is attributed to the directional bonding.

As shown in Fig. 6(b), in the strain range of 0–10 %, the length of the Fe1-Fe3 bond in the P-segregated GB model was shorter than that in the clean GB model, which results from the strong Fe-P bonds. However, after the Fe1-P bond was broken at 10–12 %, the former was longer than the latter and the breaking of the Fe1-Fe3 bond occurred at the

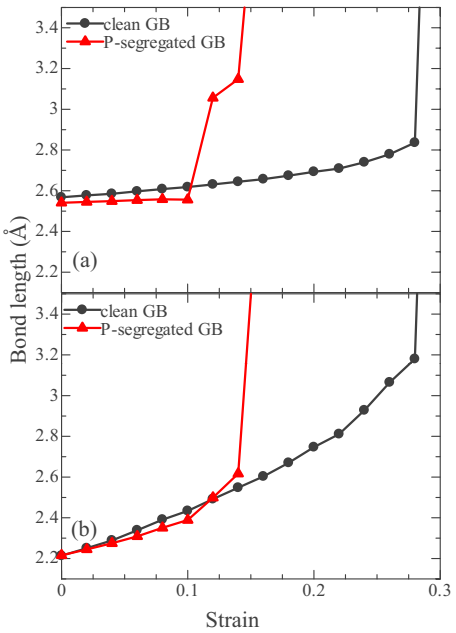


FIG. 6. (Color online) Variations in bond lengths of the (a) Fe1-Fe2/Fe1-P and (b) Fe1-Fe3 bonds as a function of strain in the clean GB and P-segregated GB models.

16%. Note that the breaking of Fe1-P bond facilitated the breaking of the Fe1-Fe3 bond in the P-segregated GB model.

Figure 7 shows the partial density of states (PDOS) for the Fe1 atom in the clean GB model and of the Fe1 and P atoms in the P-segregated GB model. The *d* electrons in the Fe1 atom in the P-segregated GB model were more localized than those in the clean GB model. Also, in the *s* and *p* electrons, hybridization peaks were observed at −13–−11 and −8–−5 eV in the Fe1 and P atoms in the P-segregated GB model. Such hybridization peaks have been reported in Fe with B- and O-segregated GBs.[22] Thus, the Fe1 atom in the P-segregated GB model exhibited covalentlike characteristics, compared with that in the clean GB model.[13] The covalentlike bonding of Fe1-P corresponds to the localized and directional charge-density states in the P-segregated GB model, as shown in Figs. 4 and 5. Ozkaya *et al.*[23] investigated the GB structure of Fe-0.4 wt % P alloy by the electron energy loss spectroscopy and they suggested that a charge transfer from P to Fe and a redistribution of electron density of Fe, which results from the flow of electrons from the *s* band to the *d* band, occur due to the electrochemical characteristics of Fe-P bond. The occupation numbers in the 3*d*, 4*s*, and 4*p* electrons of the Fe1 atom are shown in Table I. The results in Table I are consistent with the suggestions by Ozkaya *et al.*[23] It is obvious that the electrochemical characteristics are prepotent in the Fe-P bond, not the electronegativity. This is independent of the strain.

Figure 8 shows the PDOS at the strains of 10% and 14% for the Fe3 atom. The PDOS at 14% was almost the same as that at 10% in the clean GB model; however, in the P-segregated GB model, the bandwidth of *d* electrons was narrowed by increasing the strain from 10% to 14%. Also, the peak at about −2 eV in the *d* electrons was found in the PDOS at 10% and 14% in the clean GB model. However, at

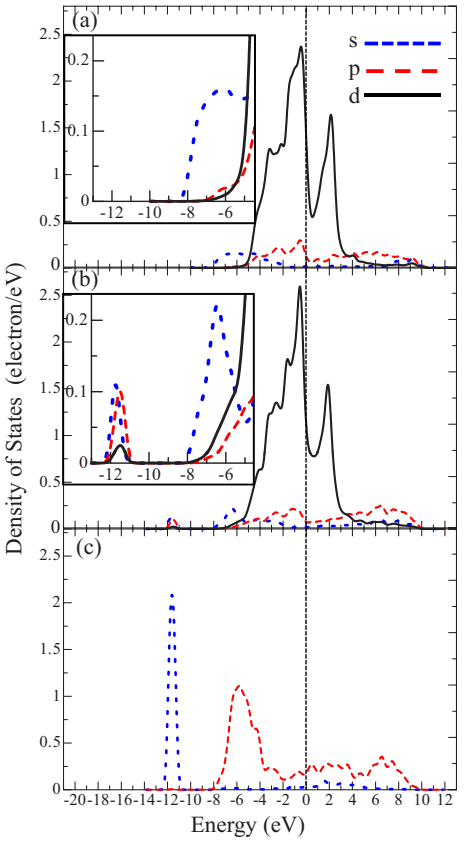


FIG. 7. (Color online) PDOS of the Fe1 and P atoms at the strain of 0%, (a) PDOS of the Fe1 atom in the clean GB model, (b) PDOS of the Fe1 atom in the P-segregated GB model, and (c) PDOS of the P atom in the P-segregated GB model. The Fermi level defines the zero of energy. The magnified figures of the PDOS in the range of −13−−5 eV are shown on the upper left.

14% in the P-segregated GB model, the peak vanished in the PDOS and the *d* electrons were more localized at the peak at −1 eV. These characteristics of the PDOS in the P-segregated GB model are related to the breaking of the Fe1-P bond at 10–12 %. Therefore, it is suggested that the breaking of the Fe1-P bond affects the electron density of states of the Fe1-Fe3 bond, accelerating the breaking of the Fe1-Fe3 bond in the P-segregated GB model.

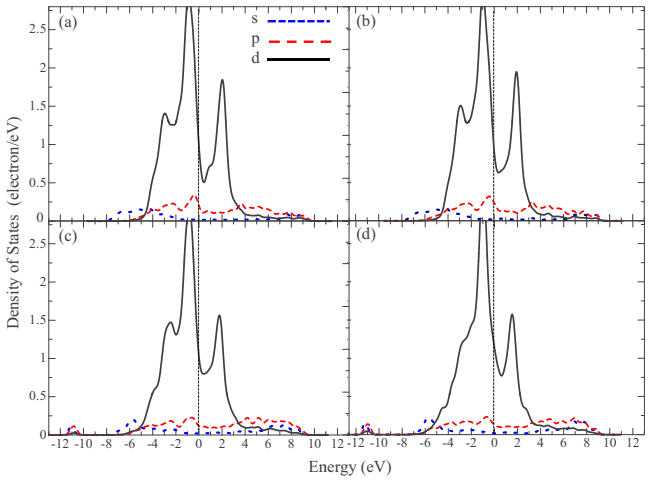


FIG. 8. (Color online) PDOS of the Fe3 atom, (a) PDOS at 10% in the clean GB model, (b) PDOS at 14% in the clean GB model, (c) PDOS at 10% in the P-segregated GB model, and (d) PDOS at 14% in the P-segregated GB model. The Fermi level defines the zero of energy.

The present study demonstrated that a strong Fe1-P bond is broken more readily than a weak Fe1-Fe2 bond owing to the reduced mobility of electrons. In the case of SiC with a GB, the weak Si-C bond is broken more readily than the strong C-C bond.[24] Also, in Al with a S-segregated GB, the weak Al-S bonds are broken readily, although the S atom is weakly bonded with some neighboring Al atoms and is strongly bonded with other Al atoms.[10] However, the present study revealed that the strong Fe-P bond is broken more readily than the weak Fe-Fe bond, and the breaking of the Fe-P bond accelerates the breaking of the Fe-Fe bond. Therefore, it is likely that the bond mobility mechanism in GB embrittlement is characterized by the easy breaking of a strong covalentlike atomic bond, and the acceleration of the breaking of a metallic bond by the breaking of a strong bond.

In conclusion, we have performed first-principles tensile tests on Fe with a P-segregated grain boundary to investigate the nature of the bond mobility mechanism in grain boundary embrittlement. Because the Fe-P bond exhibited the covalentlike characteristics, the mobility of electrons in the Fe-P bond was reduced, resulting in its easy bond breaking.

TABLE I. Occupation numbers in 3*d*, 4*s*, and 4*p* electrons of the Fe1 atom in the clean GB model and the P-segregated GB model, where the electron occupation numbers are obtained by integrated the PDOS of the Fe1 atom up to Fermi energy.

| Fe1 atom | | 3*d* | 4*s* | 4*p* | All |
|---|---|---|---|---|---|
| Clean GB model | 0% | 6.638 | 0.733 | 0.886 | 8.258 |
| | 4% | 6.629 | 0.692 | 0.916 | 8.237 |
| | 10% | 6.617 | 0.649 | 0.972 | 8.237 |
| P-segregated GB model | 0% | 6.724 | 0.698 | 0.841 | 8.263 |
| | 4% | 6.714 | 0.658 | 0.869 | 8.241 |
| | 10% | 6.695 | 0.616 | 0.895 | 8.206 |

The breaking of the Fe-P bond affected the electron density of states of the Fe-Fe bonds around the Fe-P bond, and it accelerated the Fe-Fe bond breaking. Thus, P segregation enhanced the GB embrittlement in Fe.

This work was supported from Japan Society for the Promotion of Science (Grant No. 22·5568). Computation time was provided by the SuperComputer Laboratory, Institute for Chemical Research, Kyoto University.

*Corresponding author; yuasamotohiro@t03.mbox.media.kyoto-u.ac.jp

[1] C. L. Briant and R. P. Messmer, Philos. Mag. B **42**, 569 (1980).
[2] R. P. Messmer and C. L. Briant, Acta Metall. **30**, 457 (1982).
[3] R. Haydock, J. Phys. C **14**, 3807 (1981).
[4] L. Goodwin, R. J. Needs, and V. Heine, Phys. Rev. Lett. **60**, 2050 (1988).
[5] L. Goodwin, R. J. Needs, and V. Heine, J. Phys.: Condens. Matter **2**, 351 (1990).
[6] S. Ogata, Y. Umeno, and M. Kohyama, Modell. Simul. Mater. Sci. Eng. **17**, 013001 (2009).
[7] M. Yamaguchi, M. Shiga, and H. Kaburaki, Science **307**, 393 (2005).
[8] G.-H. Lu, S. Deng, T. Wang, M. Kohyama, and R. Yamamoto, Phys. Rev. B **69**, 134106 (2004).
[9] G.-H. Lu, Y. Zhang, S. Deng, T. Wang, M. Kohyama, R. Yamamoto, F. Liu, K. Horikawa, and M. Kanno, Phys. Rev. B **73**, 224115 (2006).
[10] Y. Zhang, G.-H. Lu, S. Deng, T. Wang, H. Xu, M. Kohyama, and R. Yamamoto, Phys. Rev. B **75**, 174101 (2007).
[11] G.-H. Lu, A. Suzuki, A. Ito, M. Kohyama, and R. Yamamoto, Mater. Trans. **44**, 337 (2003).
[12] R. Wu, A. J. Freeman, and G. B. Olson, Science **265**, 376 (1994).
[13] R. Wu, A. J. Freeman, and G. B. Olson, Phys. Rev. B **50**, 75 (1994).
[14] M. Yamaguchi, Y. Nishiyama, and H. Kaburaki, Phys. Rev. B **76**, 035418 (2007).
[15] Y.-Q. Fen and C.-Y. Wang, Comput. Mater. Sci. **20**, 48 (2001).
[16] M. C. Payne, M. P. Teter, D. C. Allan, T. A. Arias, and J. D. Joannopoulos, Rev. Mod. Phys. **64**, 1045 (1992).
[17] P. Hohenberg and W. Kohn, Phys. Rev. **136**, B864 (1964).
[18] W. Kohn and L. Sham, Phys. Rev. **140**, A1133 (1965).
[19] J. P. Perdew, K. Burke, and M. Ernzerhof, Phys. Rev. Lett. **77**, 3865 (1996).
[20] D. Vanderbilt, Phys. Rev. B **41**, 7892 (1990).
[21] J. R. Rice and J.-S. Wang, Mater. Sci. Eng., A **107**, 23 (1989).
[22] Z.-Z. Chen and C.-Y. Wang, J. Phys.: Condens. Matter **17**, 6645 (2005).
[23] D. Ozkaya, J. Yuan, and L. M. Brown, in *Proceedings of the Institute of Physics Electron Microscopy and Analysis Group Conference*, Birmingham, 1995, edited by D. Cherns (University of Birmingham, Birmingham, 1995), p. 345.
[24] M. Kohyama, Philos. Mag. Lett. **79**, 659 (1999).